RADIATION-INDUCED DELAY OF NUCLEAR PORE FORMATION

JOSEPH G. SZEKELY and THEODORE P. COPPS. From the Medical Biophysics Branch, Atomic Energy of Canada Limited, Whiteshell Nuclear Research Establishment, Pinawa, Manitoba, Canada ROE 1LO

Although DNA is widely accepted as the principal radiation target in mammalian cells, some workers consider membranes to be modifiers of radiation damage, or important radiosensitive targets themselves (1, 2, 4, 13). We have measured the density of pores on nuclear envelope fragments to quantify radiation-induced membrane damage at a site intimately connected with DNA. We were motivated by the work of Zermeno and Cole (17). They explained the results of electron beam irradiation experiments by postulating that a thin peripheral shell inside the nucleus is the major radiosensitive site in the interphase Chinese hamster cell. Thus, from this interpretation, either a cellular component such as the nuclear envelope, or a small fraction of chromatin located near it is involved in radiosensitivity.

Alper has suggested that the DNA-membrane attachment site is the usual point of radiation damage in bacteria (2). Similar attachment sites have been identified in mammalian cells (12); in fact, there is evidence that pores are connected to chromatin and even carried as part of the chromosome at metaphase (5). Alkaline sucrose sedimentation patterns also show a lipid-protein-DNA complex which is broken down by radiation but is repairable by the cell (8). These observations suggest that development of the nuclear envelope through the cell cycle might be a useful indicator of radiation damage.

The nuclear envelope is a double membrane system of which the main feature is a network of pores covering its surface (Fig. 1). Pore structure has been studied extensively by electron microscopy and is usually described by general features such as an annular ring, central granule, and a circular (or octagonal) shape; however, the exact structure is still the subject of vigorous debate (9). Different preparation techniques often give conflicting pictures of pores.

The function of the pore is not completely understood, although its role in nucleus-cytoplasm communication is widely accepted. Pores may also organize the chromatin distribution within the nucleus.

When the nuclear envelope reforms after mitosis in HeLa and Chinese hamster cells, the number of pores increases through the cell cycle. The

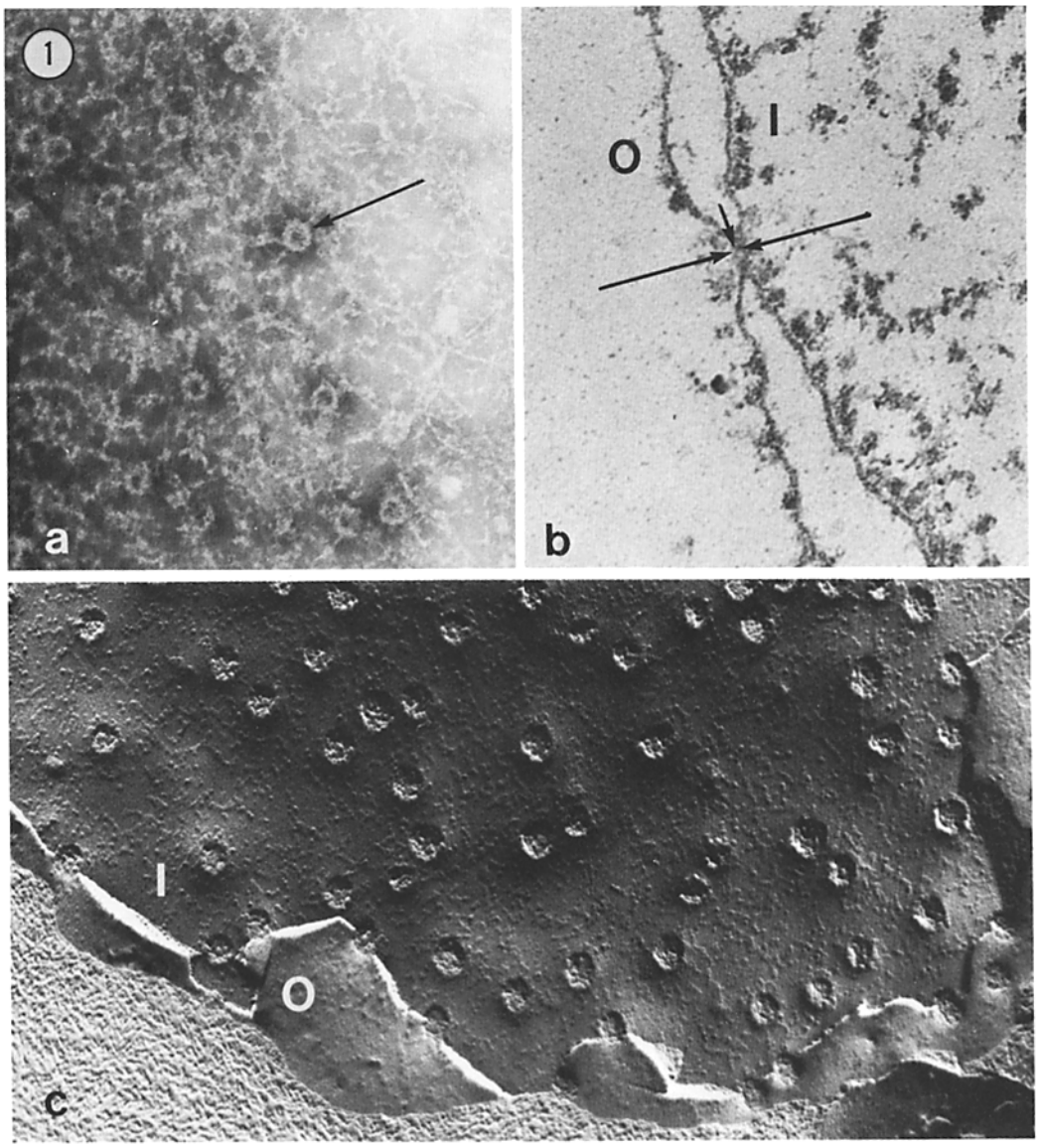

FIGURE 1 Examples of nuclear pores in Chinese hamster cells. *(a)* A nuclear envelope from a water-spread cell negatively stained with 1% ammonium molybdate. Annular rings (arrow) are visible along with connecting fibers, which appear to run along the nuclear surface. × 35,900. *(b)* Section of an Epon-embedded nucleus which had been isolated in hexylene glycol-PIPES buffer. The isolation procedure has swelled the perinuclear space, and clearly shows the double membrane structure of the nuclear envelope. The inner *(I)* and outer *(O)* membranes are continuous (arrow) in this view, although the outer membrane appears thinner in many sections. An annular structure (large arrows) with a diffuse central granule is also seen. × 107,000. *(c)* A freeze-etch picture of a nucleus viewed from the cytoplasmic side. The fracture plane follows the outer membrane *(O)* before dropping down to the inner membrane *(I)*. The view of the inner membrane emphasizes the annular ring and gives the pore structure a "crater-like" appearance. Small particles on the surface follow a pattern similar to the fibers in the negatively stained preparation. Pores visible on the outer membrane appear as definite indentations. As seen from this print, the nuclear area and pores are well defined by freeze-etching. Thus it is possible to measure pore density much more confidently than from negatively stained or sectioned material. × 43,100.

largest rate of increase is in the period of late G_1 and early S phase, perhaps reflecting a specific metabolic activity (10, 14).

Radiation effects on tissue culture cells are usually measured by one of two end-points: cell-killing, as reflected in colony formation; or mitotic delay. Delay in cell cycle progression as characterized by a delay in development of the nuclear envelope can be studied by electron microscopy using the freeze-etch technique. Freeze-etch specimens contain cells with large patches of nuclear envelope exposed, making the pores visible (Fig. 1 *c*). Thus, a delay in development of the nuclear envelope can be inferred from the pore density.

MATERIALS AND METHODS

Chinese hamster cells V79 (kindly supplied by Dr. J. D. Chapman, Whiteshell Nuclear Research Establishment) were taken from spinner culture and plated into bottles at a concentration of $2.0–3.0 \times 10^6$ cells per bottle. They were maintained overnight in Eagle's minimal essential medium supplemented with nonessential amino acids, antibiotics, and 10% fetal bovine serum. All manipulations of the cells up to the time of irradiation were carried out in a room controlled to 37°C temperature to eliminate growth delays. Cells were synchronized 15–20 h after plating by adding 0.06 μg/ml of Colcemid to 10 ml of covering medium for 2 h. The cells were harvested in fresh conditioned medium by gentle agitation on a reciprocating shaker table (140 cycles/min with a stroke length of 2 in) for 40 s. The bottles were shaken four at a time. The mitotic cell suspension from the first set of harvested cells was transferred to subsequent sets to facilitate concentrating the mitotic cells. The harvested cells were allowed to reattach on 250-ml Falcon flasks (Falcon Plastics, Oxnard, Calif.) at 37°C for 1 h before irradiation.

The cells were irradiated at room temperature in a Westinghouse 250 kV therapy unit, without filtering, at a dose rate of 570 rad/min. They were then incubated for 5 h before being processed for electron microscopy.

The cells were scraped off the flasks with a rubber policeman into Sorensen's phosphate buffer (PBS), pH 7, at room temperature, and pelleted by centrifugation. The pellet was washed twice in PBS and once in PBS + 20% glycerin for 10 min. It was then held in PBS + 20% glycerin for 1 h. A droplet of the resulting cell slurry was deposited on a specimen holder, plunged into liquid Freon 22 cooled close to its freezing point (−165°C), and then transferred directly to the stub of a Denton vacuum freeze-etch unit (Denton Vacuum Inc., Cherry Hill, N. J.), or stored in liquid nitrogen for later use.

The freeze-etch unit was evacuated below 1×10^{-6} torr and the stub temperature was maintained at −190°C. The specimen was fractured with a liquid nitrogen-cooled scalpel manipulated from outside through a universal seal, then etched by maintaining the temperature at −100°C for 2 min. Immediately after etching, the specimen was cooled and shadowed with platinum-carbon followed by the evaporation of a carbon backing film. The carbon-coated specimen was removed from the freeze-etch unit, thawed, and the replica floated onto distilled water. The replica was cleaned by transferring it onto dichromate cleaning solution for 15–30 min followed by three washes in fresh distilled water. The replica was picked up on a carbon-coated grid and examined in a Philips EM 300.

The fracture surface showed membrane faces, cross-fractured cells, and nuclear envelope fragments with pores. Only nuclear envelope fragments with a smooth appearance were used. We considered rough or bumpy nuclei to be derived from either dead cells or cells which filled with ice crystals during preparation.

RESULTS AND DISCUSSION

The mean generation time for this cell line in exponential growth as a monolayer is 9 h, with mean cell cycle phases of G_1, 1–1.5 h; S, 6–6.5 h; and G_2 + M, 1–2 h (J. D. Chapman, personal communication). Cells were irradiated in G_1 phase 1 h after they were replated. At this time, the pore density is near its minimum of 7.18 ± 0.71 pores/μm^2 as measured in separate experiments. The cells were then frozen at 6 h after replating, which puts them well into S phase if they suffer no delays due to radiation and treatment. The maximum rate of increase of pores is near the G_1-S boundary where the pore density is approaching its maximum (10, 14).

Fig. 2 shows the density of pores found on the nuclei 5 h after irradiation. The nuclear area was

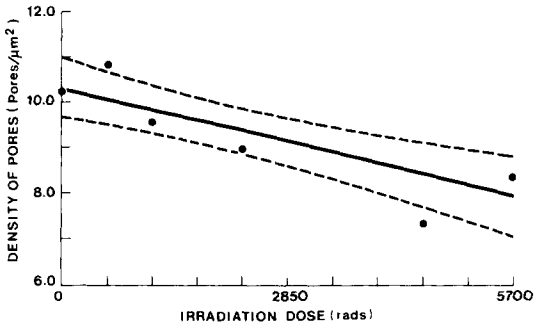

FIGURE 2 The density of pores visible on nuclear envelope fragments vs. irradiation dose. The dose rate was 570 rad/min. The least squares line $y = 10.3–4.18 \times 10^{-4}$ D which gave the best fit to the data is plotted, along with its 95% confidence interval. The confidence interval was taken as $y \pm (t(n - 2, 0.05) \times$ estimated standard error in y) (7).

TABLE I

Nuclear Pore Density in Chinese Hamster Cells after Irradiation

Dose	Pore density	Standard deviation of mean	Number of pores	Nuclear area	Number of micrographs
rad	*pore/μm²*	*pore/μm²*		*μm²*	
Control	10.28	0.55	1,137	110.6	17
570	18.81	0.36	477	44.12	6
1,140	9.51	0.16	176	18.51	4
2,280	8.94	0.50	358	40.03	6
4,560	7.34	0.43	118	16.07	4
5,700	8.36	0.29	310	37.19	10

measured by planimetry from photographs at a magnification of 54,260. The pore density is roughly inversely proportional to dose up to 5,700 rads. The pore density varies from 10.3 pores/μm^2 for control cells, which have been incubated for 6 h after mitotic selection, to 8.36 pores/μm^2 for a cell incubated for 1 h, irradiated to 5,700 rad, and then incubated for 5 h (see Table I). The points have been fitted to a straight line by the least squares method and show a decrease of 0.042 (pores/μm^2)/100 rad. We interpret this decrease as a delay in the development of the nuclear envelope, since it has a pore density appropriate for an earlier point in the cell cycle. The density can, of course, decrease as a result of either an increase in nuclear surface area or a decrease in pore number. However, measurements obtained by other investigators (10, 11) have shown that pore number, nuclear size, and pore density increase together through the cell cycle. We have assumed that this balance between nuclear size and pore number continues to hold in irradiated cells.

Once the radiation dose is large enough to completely stop development of the nuclear envelope, the pore density will remain at its minimum value. The curve in Fig. 2 is still decreasing at 5,700 rad and has not reached 7.18 pores/μm^2, the value we obtained for G_1 cells; hence, development of the nuclear envelope has not been completely stopped, even by this large dose.

The literature on mitotic and division delay contains much discussion on whether the delay occurs by proportionate lengthening of the total cycle, or principally of the G_2 phase (3, 15, 16). Our measurements show that development of the nuclear envelope is delayed even within the first 5 h, when the cells are in the early part of the cell cycle. If the pore density regulates a flow of RNA between the nucleus and cytoplasm, the decrease in density could restrict the passage of molecules through the nucleus. However, as Walters and Petersen have shown (16), recovery from division delay can occur in the absence of DNA and RNA synthesis as long as the lifetime of mRNA is not exceeded. Thus, it is doubtful that the decrease in pore density can influence the portion of the cell cycle spent in G_1 and early S.

However, the decrease in pore density can act as a significant factor in later parts of the cell cycle. A delay in pore formation which slows RNA transport will delay protein synthesis later in the cell cycle. This may account for the lengthening of G_2 often seen after irradiation (3, 15).

From the present data, it is not possible to define the site of radiation damage which leads to the decrease in the pore density that we have interpreted as a delay in the development. In all probability, it is a reflection of a general disruption of synthesis and metabolism throughout the cell. A more specific interpretation, that the decrease in pore density is due to damage to the nuclear membrane, cannot be discounted. A small permeability change, for example, induced by the radiation could cause the membrane portion of the nuclear envelope to swell in the freezing buffer, thereby reducing the pore density by increasing the area of the nuclear membrane.

SUMMARY

We have shown that radiation affects the nuclear envelope, a membrane structure closely associated with DNA. The density of nuclear pores visible on freeze-etch surfaces decreased at a rate of 0.042 (pores/μm^2)/100 rad with respect to unirradiated cells. This is interpreted as a radiation-induced delay in development of the nuclear envelope.

A preliminary account of this work appeared in Abstracts of the Microscopical Society of Canada, **2**:80–81. (see reference 6).

Received for publication 15 December 1975, and in revised form 1 April 1976.

REFERENCES

1. ALPER, T. 1973. Cell membranes as structures responsible for the oxygen effect. *In* Advances in Radiation Research, Biology and Medicine. Vol. 1. J. F. Duplan and A. Chapiro, editors. Gordon & Breach, New York. 445-456.
2. ALPER, T. 1974. The role of membrane damage in irradiated cells. Proceedings of the British Institute of Radiology. *Br. J. Radiol.* **47:**240.
3. BACCHETTI, S., and W. K. SINCLAIR. 1970. The relation of protein synthesis to radiation-induced division delay in Chinese hamster cells. *Radiat. Res.* **44:**788-806.
4. CHELACK, W. S., M. P. FORSYTH, and A. PETKAU. 1974. Radiobiological properties of Acholeplasma laidlawii B. *Can. J. Microbiol.* **20:**307-320.
5. COMINGS, D. E., and T. A. OKADA. 1970. Association of chromatin fibres with the annuli of the nuclear membrane. *Exp. Cell Res.* **62:**293-302.
6. COPPS, T. P., and J. G. SZEKELY. 1975. Radiation effects on the development of the nuclear envelope. Microsc. Soc. Can. Abstr. **2:**80-81.
7. DRAPER, N. R., and H. SMITH. 1966. Applied Regression Analysis. John Wiley & Sons, Inc., New York. 7-24.
8. ELKIND, M. M., and E. BEN-HUR. 1972. DNA lesions and mammalian cell killing: cause and effect? *Israel J. Chem.* **10:**1255-1272.
9. FRANKE, W. W., and V. SCHEER. 1974. Structures and functions of the nuclear envelope. *In* The Cell Nucleus. Vol. 1. H. Busch, editor. Academic Press, Inc., New York. 220-328.
10. MAUL, G. G., H. M. MAUL, J. E. SCOGNA, M. W. LIEBERMAN, G. S. STEIN, B. Y. HSU, and T. W. BORUN. 1972. Time sequence of nuclear pore formation in phytohemagglutinin-stimulated lymphocytes and in HeLa cells during the cell cycle. *J. Cell Biol.* **55:**433-447.
11. MAUL, H. M., B. Y. HSU, T. M. BORUN, and G. G. MAUL. 1973. Effect of metabolic inhibitors on nuclear pore formation during the HeLa S_3 cell cycle. *J. Cell Biol.* **59:**669-676.
12. O'BRIEN, R. L., A. B. SANYAL, and R. H. STANTON. 1972. Association of DNA replication with the nuclear membrane of HeLa cells. *Exp. Cell Res.* **70:**106-112.
13. PETKAU, A., and W. S. CHELACK. 1974. Protection of Acholeplasma laidlawii B by superoxide dismutase. *Int. J. Radiat. Biol.* **26:**421-426.
14. SCOTT, R. E., R. L. CARTER, and W. R. KIDWELL. 1971. Structural changes in membranes of synchronized cells demonstrated by freeze-cleavage. *Nat. New Biol.* **233:**219-220.
15. SINCLAIR, W. K. 1968. Cyclic X-ray responses in mammalian cells "in vitro." *Radiat. Res.* **33:**620-643.
16. WALTERS, R. A., and D. F. PETERSEN. 1968. Radiosensitivity of mammalian cells. II. Radiation effects on macromolecular synthesis. *Biophys. J.* **8**(12):1487-1504.
17. ZERMENO, A., and A. COLE. 1969. Radiosensitive structure of metaphase and interphase hamster cells as studied by low-voltage electron beam irradiation. *Radiat. Res.* **39:**669-684.